Optical sensing of specific molecular targets and pathways deep inside living mice has become possible as a result of a number of advances. These include design of biocompatible near-infrared fluorochromes, development of targeted and activatable 'smart' imaging probes, engineered photoproteins and advances in photon migration theory and reconstruction. Together, these advances will provide new tools making it possible to understand more fully the functioning of protein networks, diagnose disease earlier and speed along drug discovery.

Shedding light onto live molecular targets

RALPH WEISSLEDER &
VASILIS NTZIACHRISTOS

With the completion of several genome sequences, the next crucial step is to understand the function of gene products and their role in the development of disease. This knowledge will potentially facilitate the discovery of informative biomarkers that can be used for the earliest detection of disease and for the creation of new classes of drugs directed at new therapeutic targets. Thus, one of the capabilities most highly sought after is the noninvasive visualization of specific molecular targets, pathways and physiological effects *in vivo*. Revolutionary advances in fluorescent probes, photoproteins and imaging technologies have allowed cell biologists to carry out quantitative examination of cell structure and function at high spatial and temporal resolution. Indeed, whole-cell assays have become an increasingly important tool in screening and drug discovery. The rapid adaptation of these tools and the development of new tools for imaging in deep tissues in live animals is currently changing how we visualize molecular processes *in vivo* and, ultimately, clinically. The primary facilitating technologies have been progress in mathematically modeling of photon propagation in tissue, expanding availability of biologically compatible near-infrared (NIR) probes and the development of highly sensitive photon-detection technologies. In this article, we briefly review recent advances in macroscopic optical molecular imaging technologies, with a special focus on potential clinical applications.

Optical imaging techniques have used different physical parameters of light interaction with tissue (Table 1). Surface and multispectral images have been used to assess epithelial tissue structure and physiology[1–3], brain function[4,5] or superficial redox potential[6]. Probing of hemoglobins deeper in tissue has been used in functional transillumination or reflectance imaging[7,8] or diffuse optical tomography[9–14]. Other techniques have exploited light polarization[15] or light interference[16,17]. With these techniques collectively, image signal is primarily a function of 'internal contrast', and is often limited in information content (the analogy would be microscopy without stains). Two more recent techniques, however, are rapidly gaining in popularity, because they impart molecular specificity to *in vivo* imaging technologies: fluorescence and luminescence imaging. In fluorescence imaging, the energy from an external source of light is absorbed and almost immediately re-emitted at a longer, lower-energy wavelength. Fluorescence imaging can be done at different resolutions and depth penetrations, ranging from micrometers (intravital microscopy) to centimeters (fluorescence molecular tomography, FMT) (Table 1). In luminescence imaging, light is produced from a chemical reaction without an excitation light (in contrast to the absorption of photons in fluorescence). Bioluminescence is a subset of chemiluminescence, in which the light-producing chemical reaction occurs inside an organism. Irrespective of the mode of signal generation, systems suitable for use *in vivo* are those that employ compounds and reactions with high quantum yields that emit in the NIR wavelength range (Fig. 1).

Imaging in the near-infrared
Light in the visible-wavelength range is routinely used for conventional and intravital microscopy[18]. One of the key strategies for imaging deeper tissues (that is, more than a few millimeters inside the sample) has been the use of NIR light. This is because hemoglobin (the principal absorber of visible light) and water and lipids (the principal absorbers of infrared light) have their lowest absorption coefficient in the NIR region of around 650–900 nm (Fig. 1). Imaging in the NIR region has also the added advantage of minimizing tissue autofluorescence, which can further improve target/background ratios[19] (see Fig. 1, insert). Interpretation of NIR data and images generally requires advanced data processing techniques to account for the diffuse nature of photon propagation in tissue.

Several fluorescence-based imaging techniques are available (Table 1). For a review of intravital microscopy see several excellent recent review articles[18,20,21]. Macroscopic fluorescence reflectance imaging (FRI) is a useful technique when probing superficial structures (<5 mm deep), for example during endoscopy[22,23], dermatological imaging[3], intraoperative imaging[24], probing tissue autofluorescence[25,26] or small animal imaging[27]. Fluorescence molecular tomography is the newest imaging technology that has recently been shown to localize and quantify fluorescent probes three-dimensionally in deep tissues at high sensitivities[28,29] (Fig. 2). Indeed it has become possible to image (and, importantly, to quantify) fluorochrome concentrations[30,31] and (de)quenching at millimeter resolutions[28] (Fig. 3). In the near future, FMT techniques are expected to improve considerably in spatial resolution by employing higher-density measurements and advanced photon technologies, such as modulated-intensity light or a very short photon pulse. In addition, important gains are expected when the technique is combined with anatomic tomographic imaging methods such as computed X-ray tomography (CT) or magnetic resonance imaging (MRI), using the latter information for more accurate reconstructions and for projecting molecular maps onto anatomic maps. Clinical FMT imaging applications will ultimately require highly efficient photon collection systems, but penetration depths of 7–14 cm are theoretically achievable depending on tissue type.

Near-infrared fluorochromes and reporter probes
A variety of targeted (NIR fluorochrome attached to affinity ligand) and activatable imaging probes (based on fluorescence resonance energy transfer, FRET) have recently been developed (Table 2). These probes have largely been used to detect early cancers or inflammatory processes in mouse models. In the future, however, many of these probes could be developed into clinical imaging agents.

Table 1 Optical *in vivo* imaging systems[a]

| Technique	Contrast[b]	Depth	Commonly used wavelength	Clinical potential
Microscopic resolution				
Epi	A, Fl	20 µm	Visible	Experimental
Confocal	Fl	500 µm	Visible	Experimental
Two-photon	Fl	800 µm	Visible	Yes
Mesoscopic resolution				
Optical projection tomography	A, Fl	15 mm[c]	Visible	No
Optical coherence tomography	S	2 mm	Visible, NIR	Yes
Laser speckle imaging	S	1 mm	Visible, NIR	Yes
Macroscopic resolution, intrinsic contrast				
Hyperspectral imaging	A, S, Fl	<5 mm	Visible	Yes
Endoscopy	A, S, Fl	<5 mm	Visible	Yes
Polarization imaging	A, S	<1.5 cm	Visible, NIR	Yes
Fluorescence reflectance imaging (FRI)	A, Fl	<7 mm	NIR	Yes
Diffuse optical tomography (DOT)	A, Fl	<20 cm	NIR	Yes
Macroscopic resolution, molecular contrast				
Fluorescence resonance imaging (FRI)	A, Fl	<7 mm	NIR	Yes
Fluorescence molecular tomography (FMT)	Fl	<20 cm	NIR	Yes
Bioluminescence imaging (BLI)	E	<3 cm	500–600 nm	No

[a]Note that the combination of reporter probes (Table 2) and imaging system often imparts molecular specificity. [b]A, Absorption; E, emission; S, scattering; Fl, fluorescence. [c]In cleared specimen.

Detecting early cancers. A variety of reporter probes have been used for enhanced detection of early cancers, including somatostatin receptor–targeted probes[32–34], folate receptor–targeted agents[35], tumor cell–targeted agents[36–39], agents that incorporate into areas of calcification, bone formation or both[40], and agents being activated by tumor-associated proteases[41–43]. Many of these agents accumulate in (and thus enhance) tumors to a certain degree; however, FRET-based agents can yield particularly high tumor/background signal ratios because of their nondetectability in the native state. For example, recent work has shown that highly dysplastic tumoral precursors are readily detectable by targeting cathepsin B (ref. 23), a protease capable of activating a model reporter (Table 2). In this particular study, the sensitivity and specificity of optical detection of intestinal polyps were each >95%. Similar approaches may be particularly useful for early endoscopic detection and characterization of polypoid lesions as well as laparoscopic detection of residual or recurrent tumors such as ovarian cancer. These probes have also been used to detect host response, inflammation and invasion (Fig. 3).

Fig. 1 Interaction of light with tissue. The absorption coefficient of light in tissue is dependent on wavelength and results from absorbers such as hemoglobins, lipids and water. The graph is calculated assuming normally oxygenated tissue (saturation of 70%), a hemoglobin concentration of 50 mM, and a composition of 50% water and 15% lipids. The graph also lists the emission range of several common fluorochromes and luciferases used for imaging. The insert shows autofluorescence spectra obtained *in vivo* at different excitation wavelengths (obtained from ref. 84). The excitation range, denoted as λ_x, is from 337 to 610 nm, and the emission range (λ_m) is from 360 to 750 nm. Note the much lower tissue autofluorescence at longer wavelengths. The mouse images at the bottom show experimentally measured photon counts through the body of a nude mouse at 532 nm (left) and 670 nm (right). The excitation source was a point illumination placed on the posterior chest wall. Signal in the NIR range is ~4 orders of magnitude stronger for illumination in the NIR compared with illumination with green light under otherwise identical conditions, illustrating the advantages for imaging with NIR photons.

Assessment of molecular therapy. One particularly interesting application of enzyme-activatable imaging agents has been to use them as tools for objective target assessment of new therapeutic agents. In one study, the efficacy of a matrix metalloproteinase-2 (MMP-2) inhibitor at varying dosing and timing was assessed with an MMP-2-targeted imaging probe[44]. Small molecule–induced target inhibition could be externally imaged as shortly as 8 h after therapeutic drug administration. It is clear that other classes of imaging agents will be developed to image the growing array of different drug targets.

Clinical imaging. Indocyanine green (ICG), an NIR fluorochrome, is approved for clinical retinal angiography and liver function testing[45]. It is a safe imaging agent, having been used in tens of thousands of patients with a reported side effect rate of <0.15%, an extremely favorable index as compared with other reporter agents[46]. In addition, it has been used in at least one clinical study as an absorber (not a fluorochrome) for enhanced tumor detection[31]. Near-infrared fluorochromes with improved biophysical properties (solubility, quantum yield, stability, synthetic yield, conjugatability) have recently been developed[47–49] and open new avenues for high-efficiency labeling of affinity molecules. Before they can enter routine clinical use, however, these fluorochromes will need to undergo testing and receive approval from the US Food and Drug Administration.
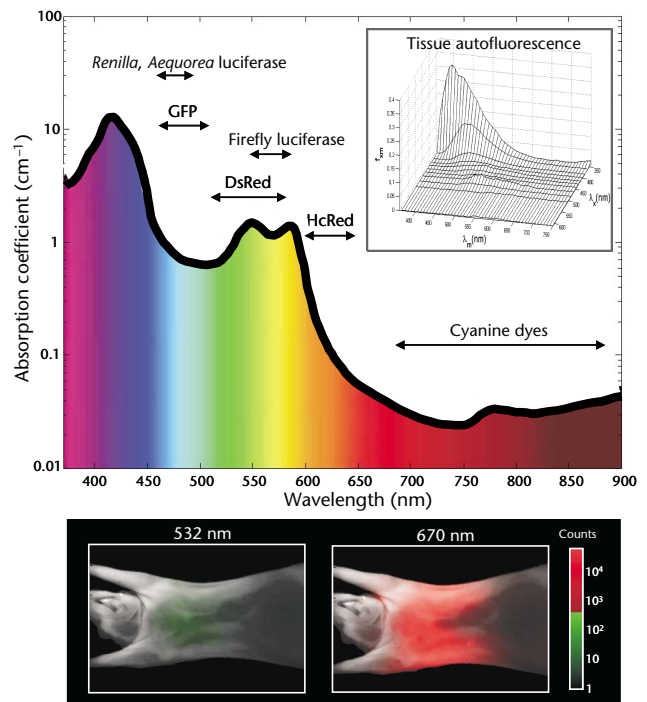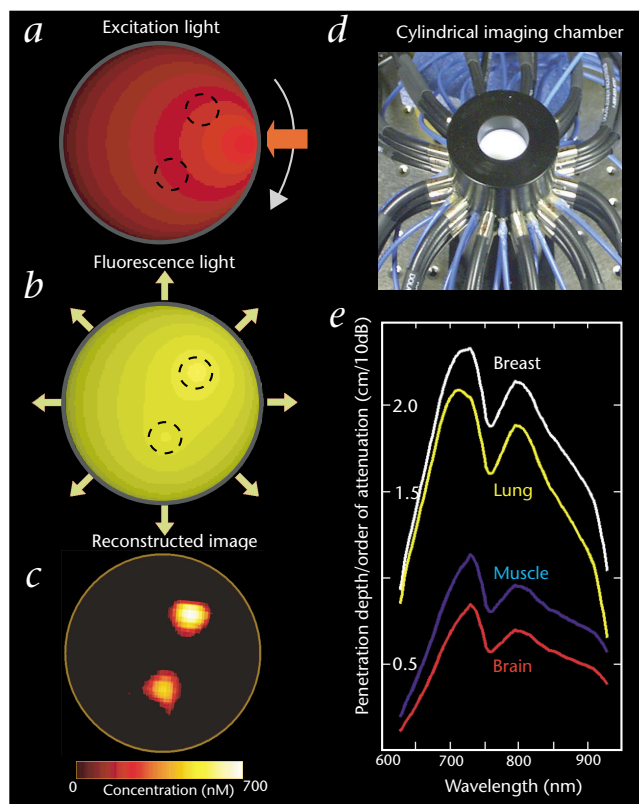
Fig. 2 Fluorescence molecular tomography. FMT is a relatively new tomographic imaging technique based on the use of target-specific molecular fluorescent reporters and volumetric reconstruction of light emitted from the probes. The imaging technique involves principles similar to X-ray CT but uses a theoretical mainframe that accounts for the diffuse nature of photons in tissues. **a**, As a single point source illuminates into tissue, the photon field will distribute as shown (isocontour lines), and excite a given distribution of fluorochromes in tissues. **b**, In each illumination position, the fluorochromes act as secondary sources at a higher wavelength, with an intensity that depends on the position of the light source. Excitation and fluorescence light are both collected from multiple points of the surface, using appropriate filters. The source then rotates around the boundary, effectively illuminating the fluorochrome distributions at different projections. **c**, The measurements are tomographically combined to yield quantitative maps of 3-dimensional (3D) fluorochrome distribution. Although the examples presented are shown in 2 dimensions only, photons propagate 3-dimensionally and thus FMT imaging is by nature 3D. **d**, An example of a cylindrical FMT imaging system for mouse imaging. Excitation (blue) and collection fibers (black) are arranged around an optical bore to deliver and collect light. FMT currently can detect nanomolar concentrations of fluorochromes at spatial resolutions of 1–2 mm in the case of small animals. Considerable penetration depths (several centimeters) can be achieved in the NIR. **e**, Modeling of the distance that NIR light can propagate into different tissues before it attenuates by an order of magnitude. Fluorochromes can be detected up to several logs of attenuations, that is, in up to 7–14 cm depth.

Fluorescent proteins

Fluorescent proteins offer another possibility for extracting molecular information in small animals but have a less defined role in clinical applications. The green fluorescent protein (GFP) from the jellyfish *Aequorea victoria* was one of the first fluorescent proteins to be used for *in vivo* imaging. A drawback of GFP is its low emission wavelength (~510 nm), which overlaps with the autofluorescence of many tissues. This is one of the reasons that mutants of GFP with red-shifted emission have been engineered, but the maximum shift attained is only ~25 nm. With any GFP, imaging is limited to a few millimeters (Fig. 1). More recently, a new red fluorescent protein (DsRed) that emits fluorescence at 583 nm has been isolated from tropical *Discosoma* corals[50]. Another red fluorescent protein that is potentially even more suitable for *in vivo* imaging is HcRed, generated by site-directed and random mutagenesis of a nonfluorescent chromoprotein isolated from the reef coral *Heteractis crispa*, which emits light at 618 nm[51,52]. Unlike bioluminescent proteins (discussed below), fluorescent proteins do not require cofactors or chemical staining before *in vivo* imaging. Much like small-molecule fluorochromes, red fluorescent proteins can be imaged quantitatively in deep tissues by FMT imaging. The ability to quantify fluorescence accurately and repeatedly will be essential in different biological applications.

Currently one of the main imaging applications of fluorescent proteins is in monitoring tumor growth[53,54] and metastasis formation[55,56], as well as occasionally gene expression[57]. Although GFP imaging of surface tumors is feasible and experimentally useful, deep-seated tumors and organ structures have to be accessed surgically for observation. For this reason, serial bioluminescence imaging of tumor burden, metastasis formation and gene expression has become more widespread. GFP-expressing tumors are particularly useful for intravital microscopy because they

Table 2 Selected optical imaging probes

Reporter	Comment
Enzyme-activatable fluorochromes	
Cathepsin B	Cancer and inflammation marker
Cathepsin K	Osteoclasts
Cathepsin D	Cancer progression
Prostate-specific antigen (PSA)	Prostate cancer
Matrix metalloproteinases (MMP-2, -9, -13)	Cancer
Cytomegalovirus (CMV)	Infection
Human immunodeficiency virus (HIV) protease	Infection
Herpes simplex virus (HSV) protease	Infection
Thrombin	Thrombosis
Caspase-1	Apoptosis
Caspase-3	Apoptosis
Targeted fluorochromes	
Phosphatidylserine	Apoptosis
Somatostatin receptor	Cancer
Anti-tumor monoclonal antibody	Cancer
Hydroxyapatite (HA)	Calcification
Glucose transporter	Cancer
Folate receptor	Cancer
Fluorescent proteins	
Green fluorescence proteins (GFPs)	480–510 nm
DsRed (from *Discosoma*)	520–580 nm
HcRed (from *Heteractis crispa*)	600–650 nm
Bioluminescent proteins	
Firefly luciferase + benzothiazole luciferin	560–610 nm emission, high QY
Renilla reniformis luciferase + coelenterazine	460–490 nm, lower QY

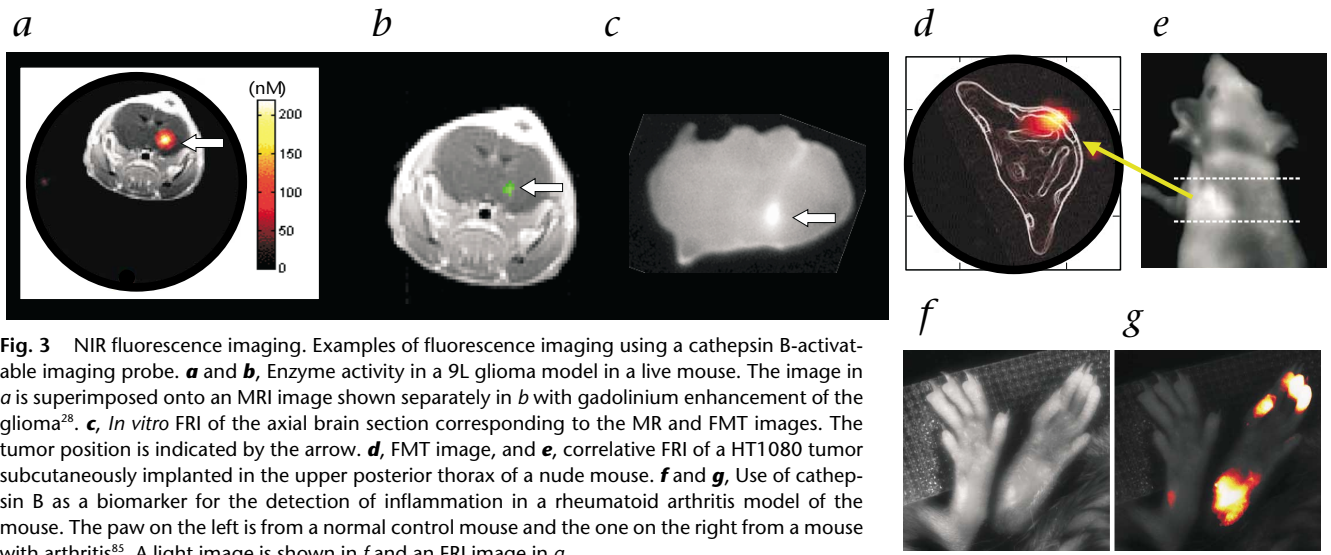See text for references. QY, quantum yield.

Fig. 3   NIR fluorescence imaging. Examples of fluorescence imaging using a cathepsin B-activatable imaging probe. **a** and **b**, Enzyme activity in a 9L glioma model in a live mouse. The image in *a* is superimposed onto an MRI image shown separately in *b* with gadolinium enhancement of the glioma[28]. **c**, *In vitro* FRI of the axial brain section corresponding to the MR and FMT images. The tumor position is indicated by the arrow. **d**, FMT image, and **e**, correlative FRI of a HT1080 tumor subcutaneously implanted in the upper posterior thorax of a nude mouse. **f** and **g**, Use of cathepsin B as a biomarker for the detection of inflammation in a rheumatoid arthritis model of the mouse. The paw on the left is from a normal control mouse and the one on the right from a mouse with arthritis[85]. A light image is shown in *f* and an FRI image in *g*.

allow clean separation between tumor and host cells[43,58]. Fluorescent proteins have also been used as reporters to image gene promoter activity[58]. Because hemoglobin is an efficient light absorber, GFP-expressing tumors have been used to image angiogenesis, as vessels are contrasted against fluorescent tumor background[59].

Bioluminescence imaging

Bioluminescence imaging has emerged as a useful and complementary experimental imaging technique for small animals. Because of its simplicity and ease of generating *luc/lux* cells, its primary uses have been for tracking tumor cells, stem cells, immune cells and bacteria as well as for imaging gene expression. In contrast to fluorescence techniques, there is no inherent background with bioluminescence, which makes this technique highly sensitive. The main limitation has been that the method currently does not allow absolute quantification of target signal. Rather, its primary uses are either in binary mode (yes/no *luc* expression) or as an imaging tool to follow the same animal under identical conditions, including positioning. The imaging signal also depends on ATP, O_2, depth and the presence of excess substrate, which is administered exogenously.

The names 'luciferin' and 'luciferase' are generic terms for the active agents (substrate and enzyme, respectively) in bioluminescent organisms[60]. Numerous examples of bioluminescence exist in nature, most notably the flashes of light emitted by the male firefly (*Photinus pyralis*). Other examples include light emission by various marine organisms such as sponges, corals, jellyfish, clams and a few types of fish. Firefly luciferin (a benzothiazole) and *P. pyralis* luciferase are the most commonly used substrate-enzyme pairs for *in vivo* imaging[61–64] because of their high wavelength and quantum yield (Table 2). More recently, imaging using *Renilla reniformis* luciferin and coelenterazine in mice has also been reported[65]. Firefly luciferin normally produces light at 562 nm, although mutants of firefly luciferase that produce red-shifted emissions have been described. Typical doses of luciferin are in large excess (120 mg/kg i.p.) and are injected immediately before data acquisition with photon-counting cameras. Image acquisition times are on the order of minutes, depending on expression levels, depth and photon flux.

One of the principal uses of luciferase imaging has been to track cells, in particular dividing cells such as tumor cells (Fig. 4)[61,66], progenitor and stem cells (Fig. 4), immune
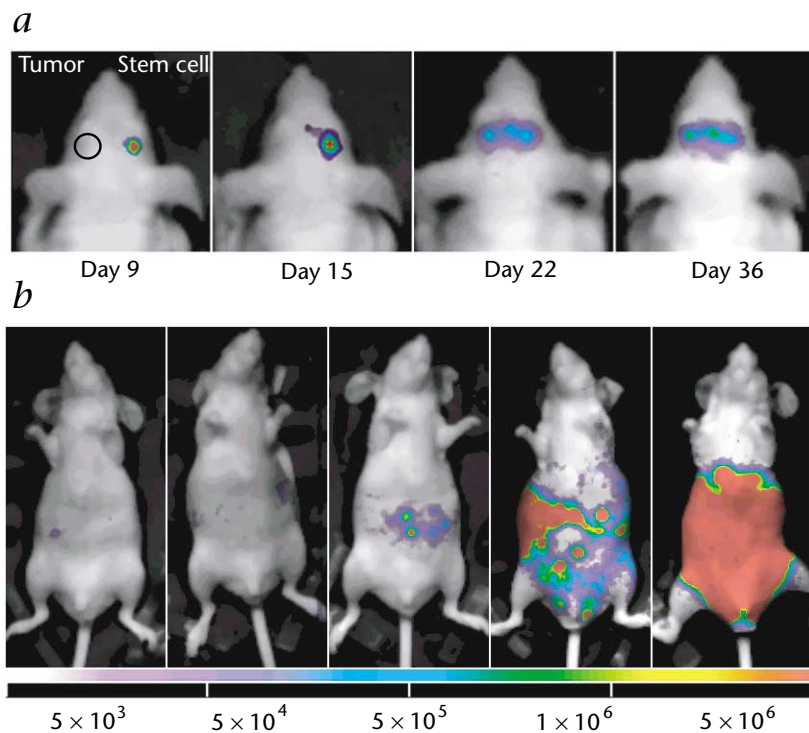

Fig. 4   Bioluminescence imaging. Two examples of imaging with bioluminescence. **a**, Migration of *luc*-labeled neural progenitor cells (C17.2, obtained from E. Snyder) across the brain midline attracted by a contralaterally implanted glioma. **b**, *Luc*-labeled OVCAR-8 ovarian cancer cells implanted into the peritoneal cavity at different densities. Note that there is a faint focus of signal even with 5×10^3 implanted cells (courtesy of Y. Tang).

cells[67] and bacterial cells[68]. Thus, for example, *luc*-expressing stem cells can be seen crossing the cerebral hemispheres in a tumor model (Fig. 4*a*), and peritoneal proliferation of ovarian cancers can be monitored over time (Fig. 4*b*). Estimates from subcutaneous implantations indicate that between 10^3 and 10^4 *luc* cells can be detected at this location. Another important application has been to use *luc* as a transgene in experimental gene transfer studies[69–71], as a screening tool for rapid identification of transgenic founder mice[72] or to visualize activation of specific pathways in cancer formation[73]. Most recently, engineered luciferases have been used to image specific cellular processes. In one study, the estrogen receptor domain was fused through a caspase-3-cleavable site to both ends of luciferase to image apoptosis *in vivo* (B. Ross, personal communication). In experimental studies, bioluminescence has been used to image protein–protein interactions[74] and NF-κB degradation[75]. It is likely that the imaging applications of luciferase will continue to expand rapidly with the use of engineered luciferases, activatable luciferins and bioluminescence resonance energy transfer (BRET) strategies.

Outlook

The next few years will bring exciting advances in imaging luminescence and fluorescence in deep organs *in vivo*—both experimentally and clinically. These advances will be based on (i) further red-shifts of probes to minimize absorption, scattering and autofluorescence; (ii) novel activatable imaging probes specific for a given target; (iii) multiwavelength imaging either to interrogate multiple targets or to implement signal correction; (iv) quantitative imaging of fluorescence through the use of photon migration theory; and (v) more sensitive detectors. It is also likely that many of these advances can and will be directly translated into clinical use, particularly the use of targeted and activatable fluorochromes. Likewise, tomographic optical imaging systems are likely to emerge and will be combined with traditional anatomic imaging methods. Another obvious clinical application is the use of endoscopes and laparoscopes as well as dermatological and other intraoperative imaging devices to sense fluorochromes at body surfaces.

On the horizon are other 'activatable' probe technologies that could ultimately be utilized *in vivo*. At the forefront are magnetic agents that change their relaxivity upon interaction with a target, either primarily spin-lattice relaxivity (R1)[76–78] or spin-spin relaxivity (R2)[79]. The latter technology is based on supramolecular assemblies of nanoparticles that change from single to oligomeric fluid phase states, accompanied by five- to tenfold changes in R2 that are easily detectable by MRI. This approach has been used to sense (and image) DNA hybridization[79], DNA methylation and cleavage[80], and protein and protease activities[81]. More recently, hybrid magnetic nanoparticle–fluorescent probes have also been developed for combined anatomic and molecular imaging in living organisms[82,83].

1. Pham, T. H. *et al*. Quantifying the absorption and reduced scattering coefficients of tissuelike turbid media over a broad spectral range with noncontact Fourier-transform hyperspectral imaging. *Appl. Opt.* **39**, 6487–6497 (2000).
2. Farkas, D.L. & Becker, D. Applications of spectral imaging: detection and analysis of human melanoma and its precursors. *Pigment Cell Res.* **14**, 2–8 (2001).
3. Zonios, G., Bykowski, J. & Kollias, N. Skin melanin, hemoglobin, and light scattering properties can be quantitatively assessed *in vivo* using diffuse reflectance spectroscopy. *J. Invest. Dermatol.* **117**, 1452–1457 (2001).
4. Gratton, G. & Fabiani, M. Shedding light on brain function: the event-related optical signal. *Trends Cogn. Sci.* **5**, 357–363 (2001).
5. Vanzetta, I. & Grinvald, A. Increased cortical oxidative metabolism due to sensory stimulation: implications for functional brain imaging. *Science* **286**, 1555–1558 (1999).
6. Piston, D.W., Masters, B.R. & Webb, W.W. Three-dimensionally resolved NAD(P)H cellular metabolic redox imaging of the *in situ* cornea with two-photon excitation laser scanning microscopy. *J. Microsc.* **178**, 20–27 (1995).
7. Franceschini, M.A. *et al*. Quantitative frequency-domain techniques enhance optical mammography: initial clinical results. *Proc. Natl. Acad. Sci. USA* **94**, 6468–6473 (1997).
8. Villringer, A. & Chance, B. Non-invasive optical spectroscopy and imaging of human brain function. *Trends Neurosci.* **20**, 435–442 (1997).
9. Benaron, D.A. *et al*. Noninvasive functional imaging of human brain using light. *J. Cerebral Blood Flow Metab.* **20**, 469–477 (2000).
10. Boas, D.A. *et al*. Imaging the body with diffuse optical tomography. *IEEE Signal Processing Mag.* **18**, 57–75 (2001).
11. Pogue, B.W. *et al*. Quantitative hemoglobin tomography with diffuse near-infrared spectroscopy: pilot results in the breast. *Radiology* **218**, 261–266 (2001).
12. Ntziachristos, V. & Chance, B. Probing physiology and molecular function using optical imaging: applications to breast cancer. *Breast Cancer Res.* **3**, 41–46 (2001).
13. Ntziachristos, V., Yodh, A.G., Schnall, M. & Chance, B. MRI-guided diffuse optical spectroscopy of malignant and benign breast lesions. *Neoplasia* **4**, 347–354 (2002).
14. Alfano, R.R. *et al*. Time-resolved and nonlinear optical imaging for medical applications. *Ann. NY Acad. Sci.* **838**, 14–28 (1998).
15. Demos, S.G., Radousky, H.B. & Alfano, R.R. Deep subsurface imaging in tissues using spectral and polarization filtering. *Optics Express* **7**, 23–28 (2000).
16. Dunn, A.K., Bolay, T., Moskowitz, M.A. & Boas, D.A. Dynamic imaging of cerebral blood flow using laser speckle. *J. Cerebral Blood Flow Metabol.* **21**, 195–201 (2001).
17. Tearney, G. *et al*. *In vivo* endoscopic optical biopsy with optical coherence tomography. *Science* **276**, 2037–2039 (1997).
18. Brown, E.B. *et al*. *In vivo* measurement of gene expression, angiogenesis and physiological function in tumors using multiphoton laser scanning microscopy. *Nat. Med.* **7**, 864–868 (2001).
19. Muller, M.G., Georgakoudi, I., Zhang, Q., Wu, J. & Feld, M.S. Intrinsic fluorescence spectroscopy in turbid media: disentangling effects of scattering and absorption. *Appl. Opt.* **40**, 4633–4646 (2001).
20. Williams, R.M., Zipfel, W.R. & Webb, W.W. Multiphoton microscopy in biological research. *Curr. Opin. Chem. Biol.* **5**, 603–608 (2001).
21. Gonzalez, S., Rajadhyaksha, M., Gonzalez-Serva, A., White, W.M. & Anderson, R.R. Confocal reflectance imaging of folliculitis *in vivo*: correlation with routine histology. *J. Cutan. Pathol.* **26**, 201–205 (1999).
22. Ito, S. *et al*. Detection of human gastric cancer in resected specimens using a novel infrared fluorescent anti-human carcinoembryonic antigen antibody with an infrared fluorescence endoscope *in vitro*. *Endoscopy* **33**, 849–853 (2001).
23. Marten, K. *et al*. Detection of dysplastic intestinal adenomas using enzyme-sensing molecular beacons in mice. *Gastroenterology* **122**, 406–414 (2002).
24. Kuroiwa, T., Kajimoto, Y. & Ohta, T. Development and clinical application of near-infrared surgical microscope: preliminary report. *Minim. Invasive Neurosurg.* **44**, 240–242 (2001).
25. Richards-Kortum, R. & Sevick-Muraca, E. Quantitative optical spectroscopy for tissue diagnosis. *Annu. Rev. Physical Chem.* **47**, 555–606 (1996).
26. Wang, T.D. *et al*. *In vivo* identification of colonic dysplasia using fluorescence endoscopic imaging. *Gastrointest. Endosc.* **49**, 447–455 (1999).
27. Mahmood, U., Tung, C.H., Bogdanov, A., Jr. & Weissleder, R. Near-infrared optical imaging of protease activity for tumor detection. *Radiology* **213**, 866–870 (1999).
28. Ntziachristos, V., Tung, C., Bremer, C. & Weissleder, R. Fluorescence-mediated tomography resolves protease activity *in vivo*. *Nat. Med.* **8**, 575–560 (2002).
29. Ntziachristos, V. & Weissleder, R. Charge-coupled-device based scanner for tomography of fluorescent near-infrared probes in turbid media. *Med. Phys.* **29**, 803–809 (2002).
30. Hawrysz, D.J. & Sevick-Muraca, E.M. Developments toward diagnostic breast cancer imaging using near-infrared optical measurements and fluorescent contrast agents. *Neoplasia* **2**, 388–417 (2000).
31. Ntziachristos, V., Yodh, A.G., Schnall, M. & Chance, B. Concurrent MRI and diffuse optical tomography of breast after indocyanine green enhancement. *Proc. Natl. Acad. Sci. USA* **97**, 2767–2772 (2000).
32. Achilefu, S., Dorshow, R.B., Bugaj, J.E. & Rajagopalan, R. Novel receptor-targeted fluorescent contrast agents for *in vivo* tumor imaging. *Invest. Radiol.* **35**, 479–485 (2000).
33. Licha, K. *et al*. Synthesis, characterization, and biological properties of cyanine-labeled somatostatin analogues as receptor-targeted fluorescent probes. *Bioconjug. Chem.* **12**, 44–50 (2001).
34. Becker, A. *et al*. Receptor-targeted optical imaging of tumors with near-infrared fluorescent ligands. *Nat. Biotechnol.* **19**, 327–331 (2001).
35. Tung, C.H., Lin, Y., Moon, W. & Weissleder, R. Receptor-targeted near-infrared fluorescence probe for *in vivo* tumor detection. *ChemBioChem* **3**, 784–786 (2002).
36. Ballou, B. *et al*. Tumor labeling *in vivo* using cyanine-conjugated monoclonal antibodies. *Cancer Immunol. Immunother.* **41**, 257–263 (1995).
37. Neri, D. *et al*. Targeting by affinity-matured recombinant antibody fragments on an angiogenesis-associated fibronectin isoform. *Nat. Biotechnol.* **15**, 1271–1275 (1997).
38. Muguruma, N. *et al*. Antibodies labeled with fluorescence-agent excitable by infrared rays. *J. Gastroenterol.* **33**, 467–471 (1998).

39. Folli, S. *et al.* Antibody–indocyanin conjugates for immunophotodetection of human squamous cell carcinoma in nude mice. *Cancer Res.* **54**, 2643–2649 (1994).

40. Zaheer, A. *et al. In vivo* near-infrared fluorescence imaging of osteoblastic activity. *Nat. Biotechnol.* **19**, 1148–1154 (2001).

41. Weissleder, R., Tung, C.H., Mahmood, U. & Bogdanov, A., Jr. *In vivo* imaging of tumors with protease-activated near-infrared fluorescent probes. *Nat. Biotechnol.* **17**, 375–378 (1999).

42. Tung, C.H., Mahmood, U., Bredow, S. & Weissleder, R. *In vivo* imaging of proteolytic enzyme activity using a novel molecular reporter. *Cancer Res.* **60**, 4953–4958 (2000).

43. Bogdanov, A.A., Jr., Lin, C.P., Simonova, M., Matuszewski, L. & Weissleder, R. Cellular activation of the self-quenched fluorescent reporter probe in tumor microenvironment. *Neoplasia* **4**, 228–236 (2002).

44. Bremer, C., Tung, C.H. & Weissleder, R. *In vivo* molecular target assessment of matrix metalloproteinase inhibition. *Nat. Med.* **7**, 743–748 (2001).

45. Slakter, J.S., Yannuzzi, L.A., Guyer, D.R., Sorenson, J.A. & Orlock, D. A. Indocyanine-green angiography. *Curr. Opin. Ophthalmol.* **6**, 25–32 (1995).

46. Hope-Ross, M. *et al.* Adverse reactions due to indocyanine green. *Ophthalmology* **101**, 529–533 (1994).

47. Riefke, B., Licha, K., Semmler, W., Nolte, D. & Rinneberg, H. *In vivo* characterization of cyanine dyes as contrast agents for near-infrared imaging. *SPIE* **2927**, 199–208 (1996).

48. Licha, K. *et al.* Hydrophilic cyanine dyes as contrast agents for near-infrared tumor imaging: synthesis, photophysical properties and spectroscopic *in vivo* characterization. *Photochem. Photobiol.* **72**, 392–398 (2000).

49. Lin, Y., Weissleder, R. & Tung, C.H. Novel near-infrared cyanine fluorochromes: synthesis, properties, and bioconjugation. *Bioconjug. Chem.* **13**, 605–610 (2002).

50. Matz, M.V. *et al.* Fluorescent proteins from nonbioluminescent *Anthozoa* species. *Nat. Biotechnol.* **17**, 969–973 (1999).

51. Gurskaya, N.G. *et al.* GFP-like chromoproteins as a source of far-red fluorescent proteins. *FEBS Lett.* **507**, 16–20 (2001).

52. Labas, Y.A. *et al.* Diversity and evolution of the green fluorescent protein family. *Proc. Natl. Acad. Sci. USA* **99**, 4256–4261 (2002).

53. Hoffman, R.M. Visualization of GFP-expressing tumors and metastasis *in vivo. Biotechniques* **30**, 1016–1022, 1024–1026 (2001).

54. Yang, M. *et al.* Whole-body optical imaging of green fluorescent protein–expressing tumors and metastases. *Proc. Natl. Acad. Sci. USA* **97**, 1206–1211 (2000).

55. Moore, A., Sergeyev, N., Bredow, S. & Weissleder, R. A model system to quantitate tumor burden in locoregional lymph nodes during cancer spread. *Invasion Metastasis* **18**, 192–197 (1998).

56. Wunderbaldinger, P., Josephson, L., Bremer, C., Moore, A. & Weissleder, R. Detection of lymph node metastases by contrast-enhanced MRI in an experimental model. *Magn. Reson. Med.* **47**, 292–297 (2002).

57. Yang, M., Baranov, E., Moossa, A.R., Penman, S. & Hoffman, R.M. Visualizing gene expression by whole-body fluorescence imaging. *Proc. Natl. Acad. Sci. USA* **97**, 12278–12282 (2000).

58. Fukumura, D. *et al.* Tumor induction of VEGF promoter activity in stromal cells. *Cell* **94**, 715–725 (1998).

59. Moore, A., Marecos, E., Simonova, M., Weissleder, R. & Bogdanov, A., Jr. Novel gliosarcoma cell line expressing green fluorescent protein: a model for quantitative assessment of angiogenesis. *Microvasc. Res.* **56**, 145–153 (1998).

60. Hastings, J.W. Chemistries and colors of bioluminescent reactions: a review. *Gene* **173**, 5–11 (1996).

61. Contag, C.H., Jenkins, D., Contag, P.R. & Negrin, R.S. Use of reporter genes for optical measurements of neoplastic disease *in vivo. Neoplasia* **2**, 41–52 (2000).

62. Contag, C.H. *et al.* Visualizing gene expression in living mammals using a bioluminescent reporter. *Photochem. Photobiol.* **66**, 523–531 (1997).

63. Contag, C.H. & Stevenson, D.K. *In vivo* patterns of heme oxygenase-1 transcription. *J. Perinatol.* **21** (Suppl. 1), S119–124; discussion S125–127 (2001).

64. Contag, P., Olomu, I., Stevenson, D. & Contag, C. Bioluminescent indicators in living mammals. *Nat. Med.* **4**, 245–247 (1998).

65. Bhaumik, S. & Gambhir, S.S. Optical imaging of *Renilla* luciferase reporter gene expression in living mice. *Proc. Natl. Acad. Sci. USA* **99**, 377–382 (2002).

66. Wetterwald, A. *et al.* Optical imaging of cancer metastasis to bone marrow: a mouse model of minimal residual disease. *Am. J. Pathol.* **160**, 1143–1153 (2002).

67. Costa, G.L. *et al.* Adoptive immunotherapy of experimental autoimmune encephalomyelitis via T-cell delivery of the IL-12 p40 subunit. *J. Immunol.* **167**, 2379–2387 (2001).

68. Burns, S.M. *et al.* Revealing the spatiotemporal patterns of bacterial infectious diseases using bioluminescent pathogens and whole body imaging. *Contrib. Microbiol.* **9**, 71–88 (2001).

69. Weng, Y.H., Tatarov, A., Bartos, B.P., Contag, C.H. & Dennery, P.A. HO-1 expression in type II pneumocytes after transpulmonary gene delivery. *Am. J. Physiol. Lung Cell Mol. Physiol.* **278**, L1273–1279 (2000).

70. Wu, J.C., Sundaresan, G., Iyer, M. & Gambhir, S.S. Noninvasive optical imaging of firefly luciferase reporter gene expression in skeletal muscles of living mice. *Mol. Ther.* **4**, 297–306 (2001).

71. Honigman, A. *et al.* Imaging transgene expression in live animals. *Mol. Ther.* **4**, 239–249 (2001).

72. Zhang, W. *et al.* Rapid *in vivo* functional analysis of transgenes in mice using whole body imaging of luciferase expression. *Transgenic Res.* **10**, 423–434 (2001).

73. Vooijs, M., Jonkers, J., Lyons, S. & Berns, A. Noninvasive imaging of spontaneous retinoblastoma pathway-dependent tumors in mice. *Cancer Res.* **62**, 1862–1867 (2002).

74. Ray, P. *et al.* Noninvasive quantitative imaging of protein–protein interactions in living subjects. *Proc. Natl. Acad. Sci. USA* **99**, 3105–3110 (2002).

75. Carlsen, H., Moskaug, J.O., Fromm, S.H. & Blomhoff, R. *In vivo* imaging of NF-κB activity. *J. Immunol.* **168**, 1441–1446 (2002).

76. Louie, A.Y. *et al. In vivo* visualization of gene expression using magnetic resonance imaging. *Nat. Biotechnol.* **18**, 321–325 (2000).

77. Moats, R.A., Fraser, S.E. & Meade, T.J. A "smart" magnetic resonance imaging agent that reports on specific enzymatic activity. *Angew. Chem. Int. Edn. Engl.* **36**, 726–731 (1997).

78. Bogdanov, A., Matuszewski, L., Bremer, C., Petrovsky, A. & Weissleder, R. Oligomerization of paramagnetic substrates result in signal amplification and can be used for MR imaging of molecular targets. *Molec. Imag.* **1**, 1–9 (2002).

79. Josephson, L., Perez, J. & Weissleder, R. Magnetic nanosensors for the detection of oligonucleotide sequences. *Angew. Chem. Int. Edn. Engl.* **40**, 3204–3206 (2001).

80. Perez, J.M., O'Loughin, T., Simeone, F.J., Weissleder, R. & Josephson, L. DNA-based magnetic nanoparticle assembly acts as a magnetic relaxation nanoswitch allowing screening of DNA-cleaving agents. *J. Am. Chem. Soc.* **124**, 2856–2857 (2002).

81. Perez, J.M., Josephson, L., O'Loughin, T., Hogeman, D. & Weissleder, R. Magnetic relaxation switches capable of sensing molecular interactions. *Nat. Biotechnol.* **20**, 816–820 (2002).

82. Josephson, L., Kircher, M. F., Mahmood, U., Tang, Y. & Weissleder, R. Near-infrared fluorescent nanoparticles as combined MR/optical imaging probes. *Bioconjug. Chem.* **13**, 554–560 (2002).

83. Huber, M.M. *et al.* Fluorescently detectable magnetic resonance imaging agents. *Bioconjug. Chem.* **9**, 242–249 (1998).

84. Georgakoudi, I., Mueller, M.G. & Feld, M.S. Intrinsic fluorescence spectroscopy of biological tissue in *Fluorescence in Biomedicine* (Marcel Dekker, New York, 2002).

85. Ji, H. *et al.* Arthritis critically dependent on innate immune system players. *Immunity* **16**, 157–168 (2002).

Center for Molecular Imaging Research, Massachusetts General Hospital and Harvard Medical School, Charlestown, Massachusetts, USA

Correspondence should be addressed to R.W;

email: weissleder@helix.mgh.harvard.edu